Supplementary Material for

Mixed-ligand copper(II) Schiff base complexes: the role of co-ligand in DNA binding, DNA cleavage, protein binding and cytotoxicity.

Wen-Jing Lian, †[a] Xin-Tian Wang, †[a] Cheng-Zhi Xie,[a] He Tian, [a] Xue-Qing Song, [a] He-Ting Pan, [a] Xin Qiao, *[a] and Jing-Yuan Xu,*[a]

[a] *Tianjin Key Laboratory on Technologies Enabling Development of Clinical Therapeutics and Diagnostics, School of Pharmacy, Tianjin Medical University, Tianjin 300070, P. R. China.*

† *Both authors contributed equally to this work.*

*__Corresponding author:__

Tel: +86 22 83336658;

E-mail: xujingyuan@tmu.edu.cn (Prof. J.-Y. Xu), qiaoxin@tmu.edu.cn(Dr. X. Qiao)

Table S1. Hydrogen binding arrangements /Å, ° for compounds **1**-**4**.

	D-H...A	*d* (H...A)	*d* (D...A)	< (DHA)	Symmetry code
1	O(2)-H(2B)...O(4)	1.86	2.672(3)	173.1	
	O(5)-H(5B)...O(1)	2.087(16)	2.921(3)	165(5)	
	N(2)-H(2C)...O(4)	2.25	3.005(3)	140.0	x,y-1,z
	N(2)-H(2C)...O(5)	2.31	2.973(3)	129.8	x,y-1,z
	O(5)-H(5C)...O(3)	2.151(14)	2.996(3)	171(6)	x+1/2,y+1/2,z
2	N(3)-H(3C) ...O(4)	1.89	2.789(2)	174.9	-x+1,-y+2,-z+1
	N(3)-H(3B) ...O(5)	1.95	2.808(2)	158.7	-x+1,y-1/2,-z+3/2
	N(3)-H(3B) ...O(6)	2.45	3.043(2)	123.5	-x+1,y-1/2,-z+3/2
3	O(2)-H(2B)...O(1)	2.05	2.8675(18)	175.6	x,-y+1,z+1/2
	N(2)-H(2C)...O(4)	2.12(2)	2.8351(18)	158(2)	x,-y,z+1/2
4	O(5)-H(5B)...O(1)	2.11	2.9310(17)	173.8	x,-y+1,z+1/2
	N(2)-H(2B)...O(3)	2.27(2)	2.8884(17)	150(2)	x,-y+2,z+1/2

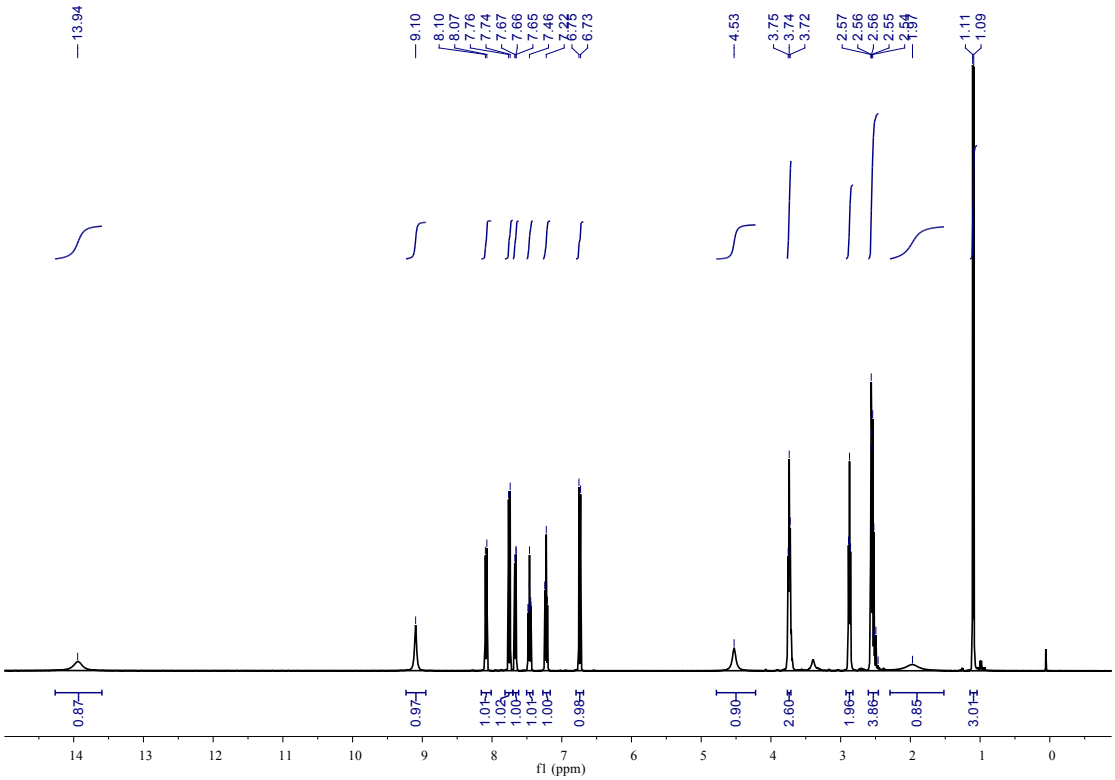

Fig. S1 ^{1}H NMR spectrum of HL

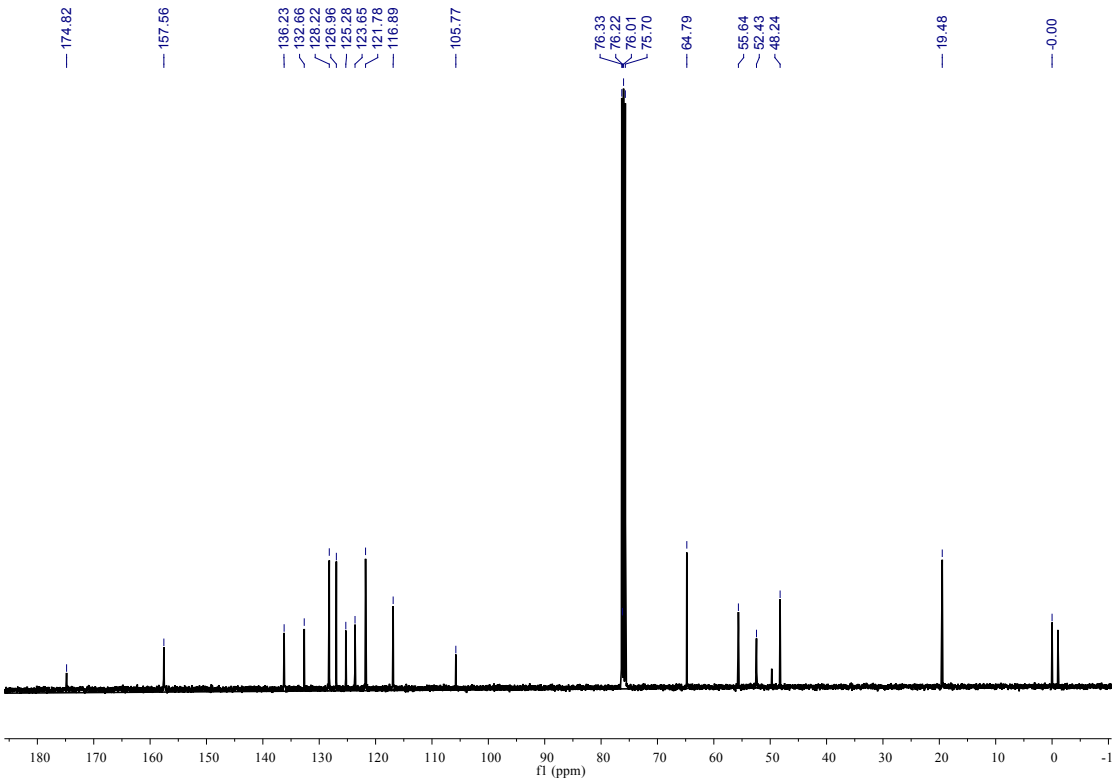

Fig. S2 ^{13}C NMR spectrum of HL

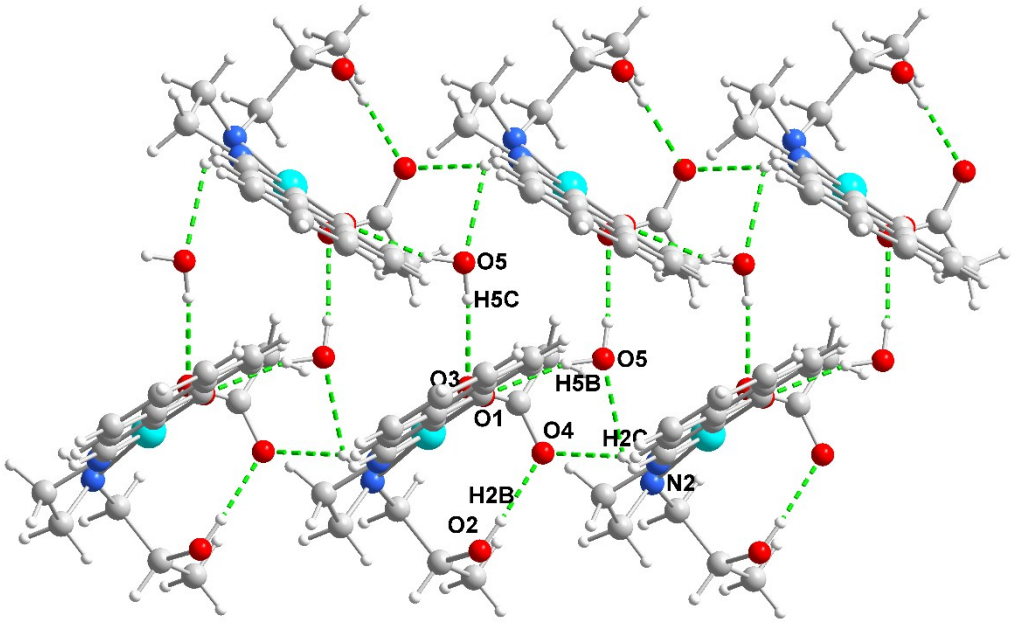

Fig. S3 Intermolecular association of complex **1**. Hydrogen bonds are marked by dashed lines.

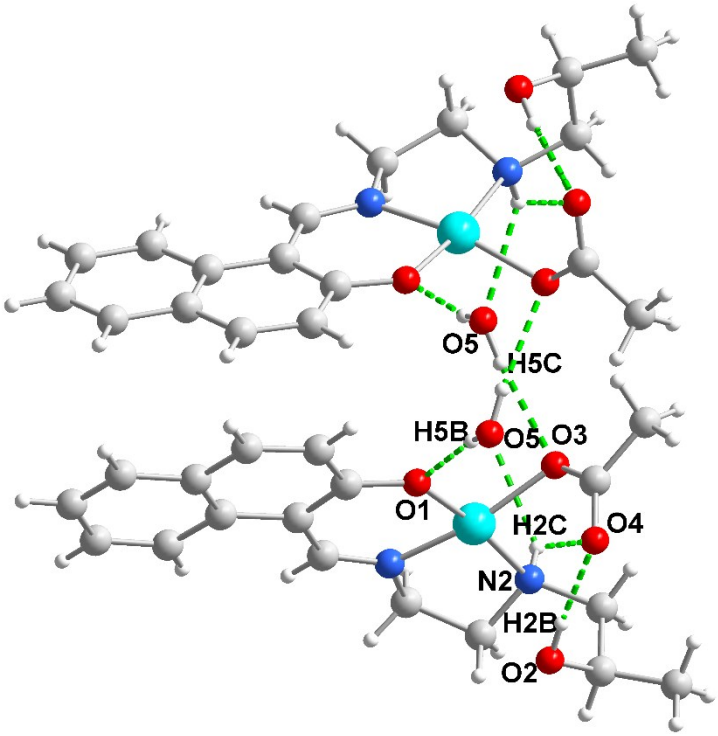

Fig. S4 Intermolecular association of complex **1**. Hydrogen bonds are marked by dashed lines.

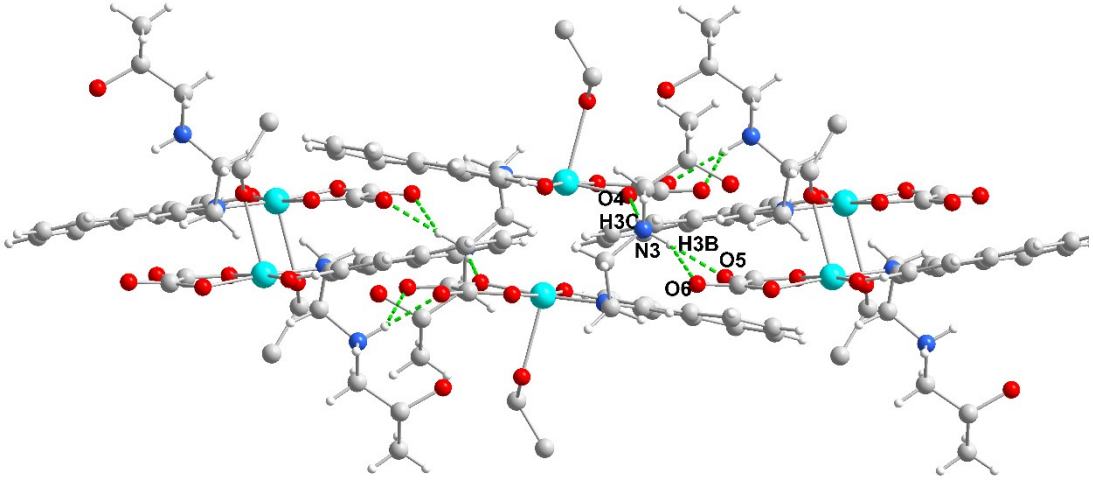

Fig. S5. Intermolecular association of complex **2**. Hydrogen bonds are marked by dashed lines.

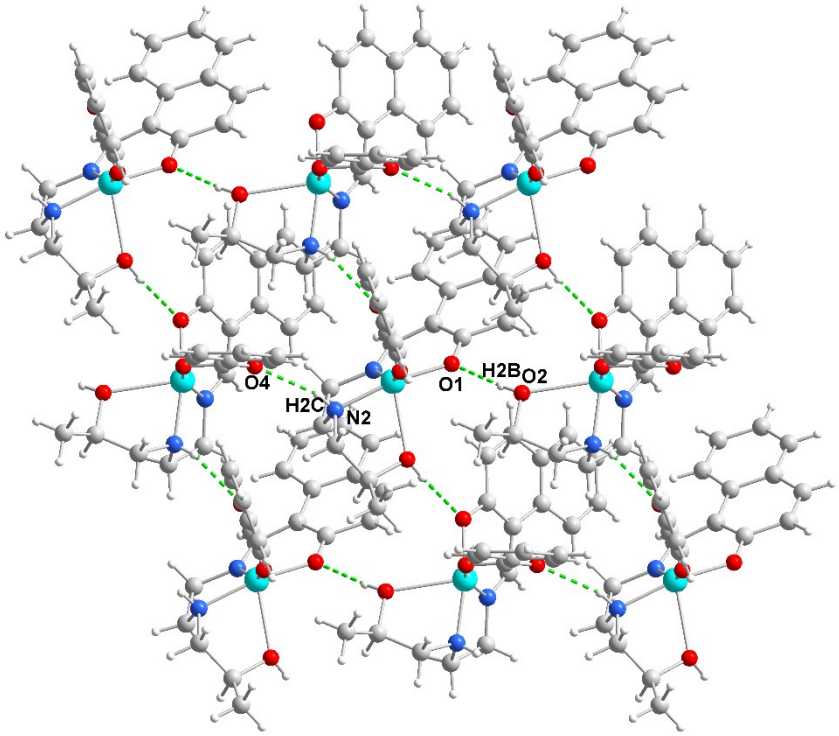

Fig. S6. Intermolecular association of complex **3**. Hydrogen bonds are marked by dashed lines.

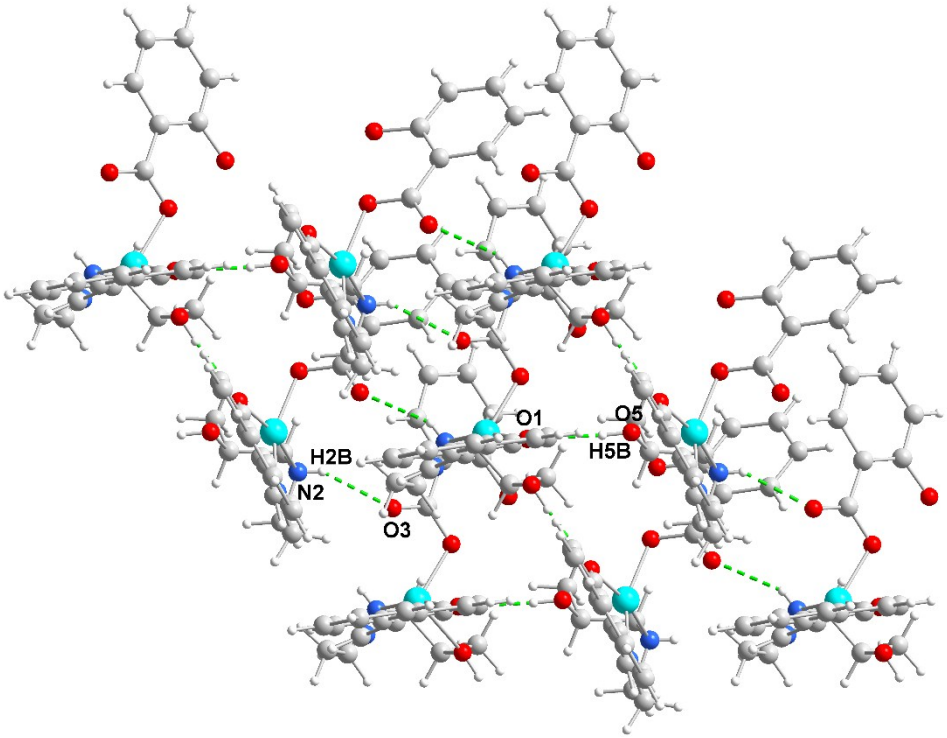

Fig. S7. Intermolecular association of complex **4**. Hydrogen bonds are marked by dashed lines.

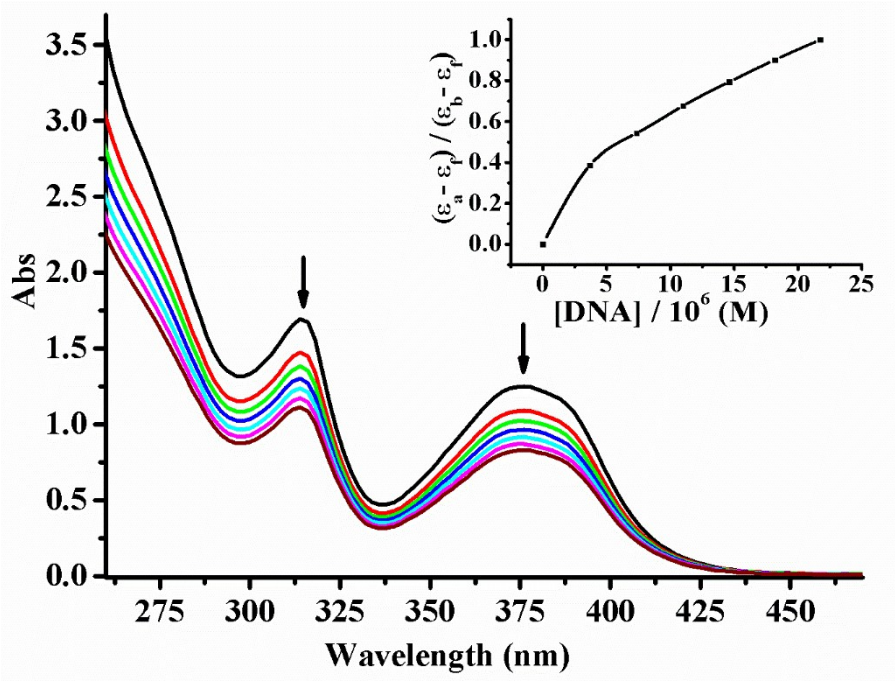

Fig. S8 Absorption spectra of complex **2** (200 μM) in the absence ((black line)) and presence (other lines) of increasing amounts of CT-DNA (7.35, 11.0, 14.6, 18.2 and 21.7 μM) at room temperature in Tris-HCl/NaCl buffer (pH = 7.2). Inset: plot of $(\varepsilon_a-\varepsilon_f)$ / $(\varepsilon_b-\varepsilon_f)$ vs. [DNA] for absorption titration of CT-DNA with complex.

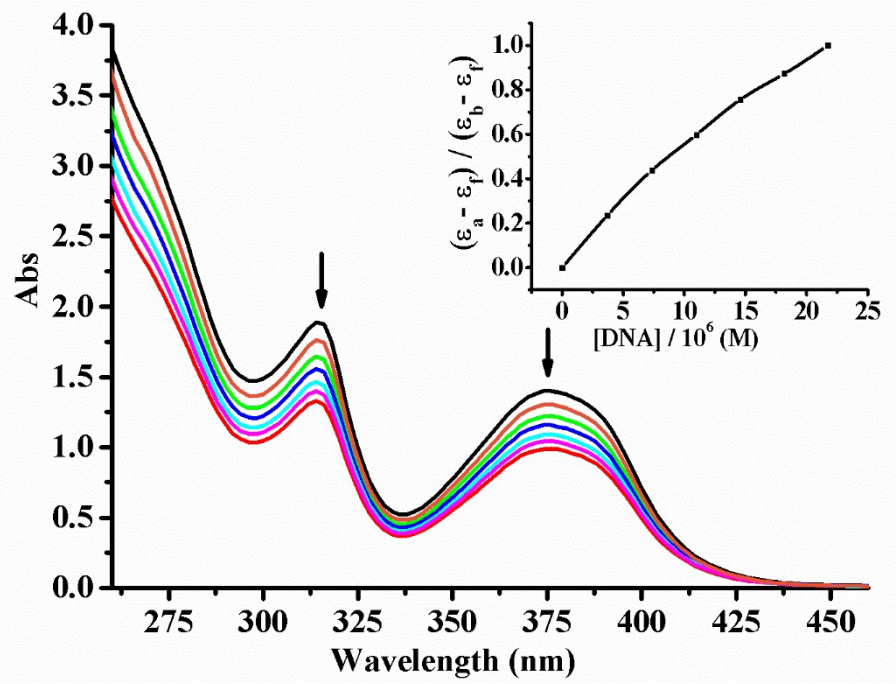

Fig. S9 Absorption spectra of complex **3** (200 μM) in the absence ((black line)) and presence (other lines) of increasing amounts of CT-DNA (7.35, 11.0, 14.6, 18.2 and 21.7 μM) at room temperature in Tris-HCl/NaCl buffer (pH = 7.2). Inset: plot of $(\varepsilon_a-\varepsilon_f)$ / $(\varepsilon_b-\varepsilon_f)$ vs. [DNA] for absorption titration of CT-DNA with complex.

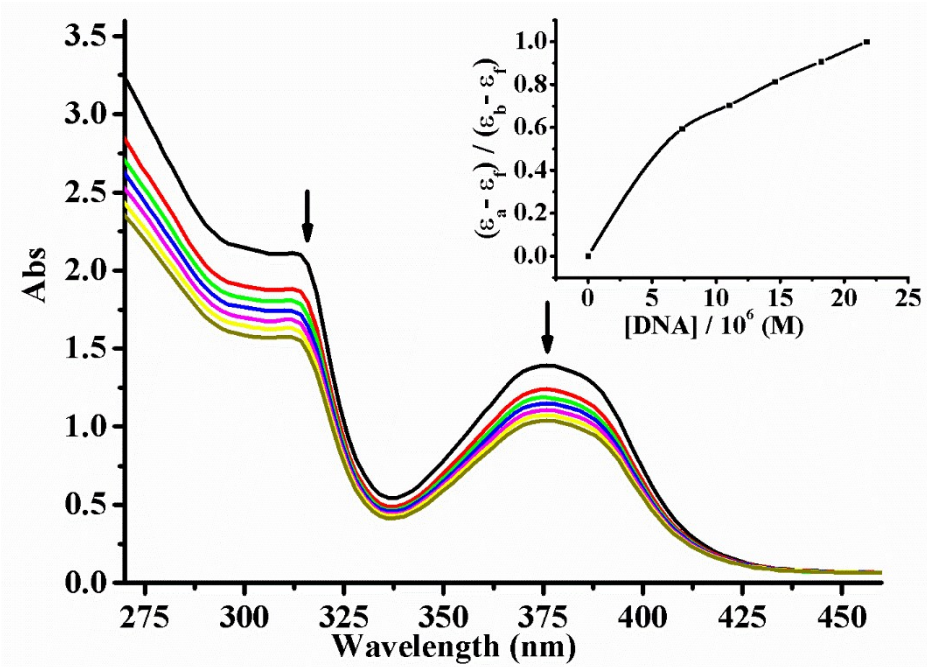

Fig. S10 Absorption spectra of complex **4** (200 μM) in the absence ((black line)) and presence (other lines) of increasing amounts of CT-DNA (7.35, 11.0, 14.6, 18.2 and 21.7 μM) at room temperature in Tris-HCl/NaCl buffer (pH = 7.2). Inset: plot of $(\varepsilon_a-\varepsilon_f) / (\varepsilon_b-\varepsilon_f)$ vs. [DNA] for absorption titration of CT-DNA with complex.

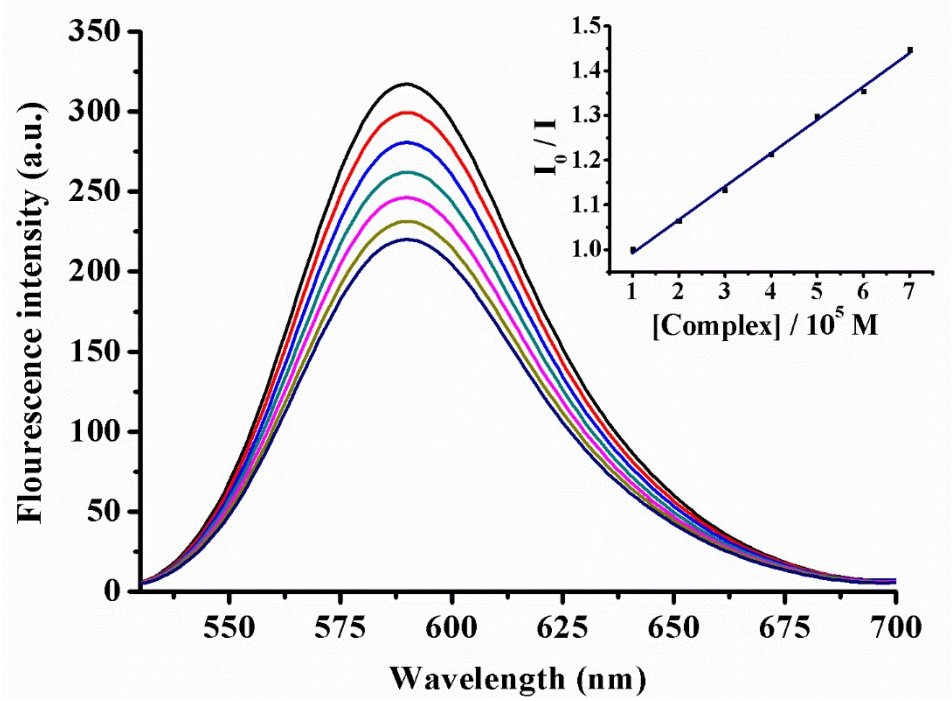

Fig. S11 Fluorescence quenching curves of EB bound to CT-DNA by complex **2** ([complex] = 0 – 70 μM, λ_{ex} = 510 nm). The arrow shows the intensity changes on increasing the complex concentration. Inset: plot of I_0/I vs. [complex].

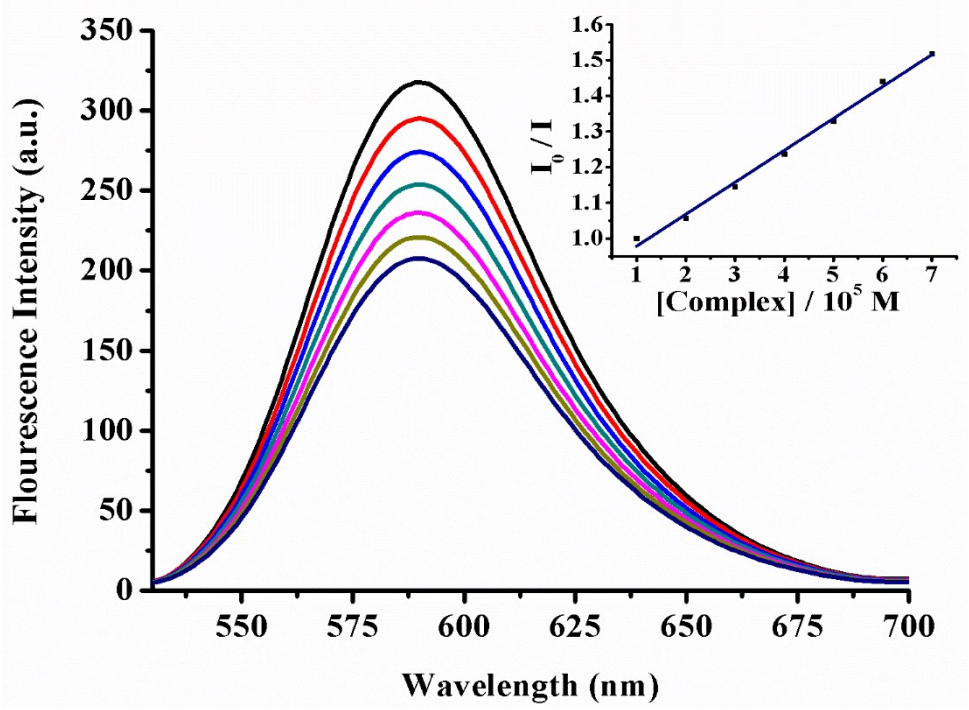

Fig. S12 Fluorescence quenching curves of EB bound to CT-DNA by complex **3** ([complex] = 0 – 70 μM, λ_{ex} = 510 nm). The arrow shows the intensity changes on increasing the complex concentration. Inset: plot of I_0/I vs. [complex].

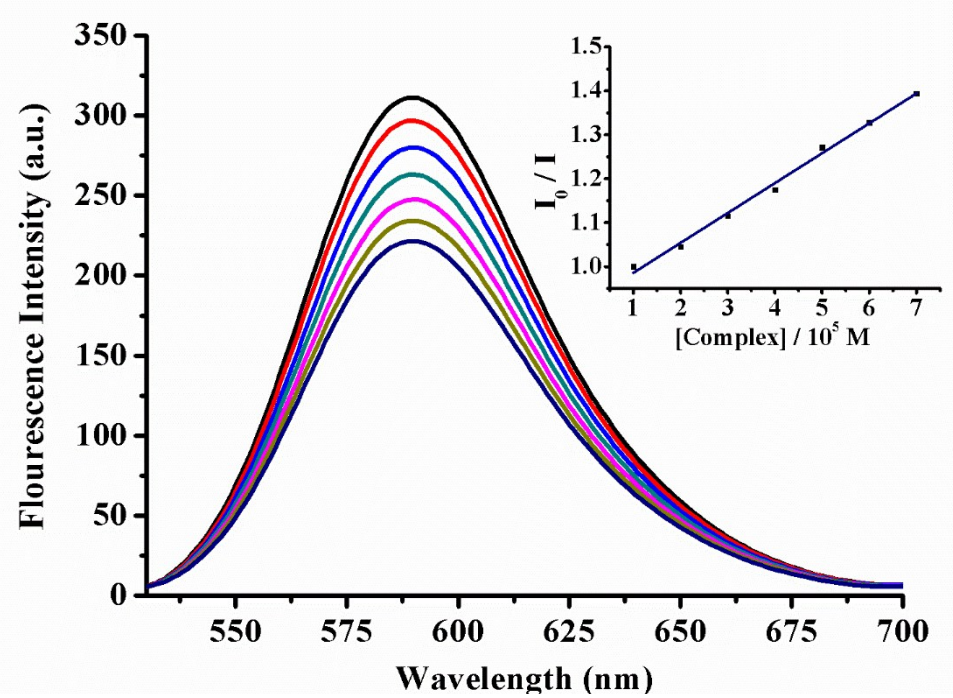

Fig. S13 Fluorescence quenching curves of EB bound to CT-DNA by complex **4** ([complex] = 0 – 70 μM, λ_{ex} = 510 nm). The arrow shows the intensity changes on increasing the complex concentration. Inset: plot of I_0/I vs. [complex].

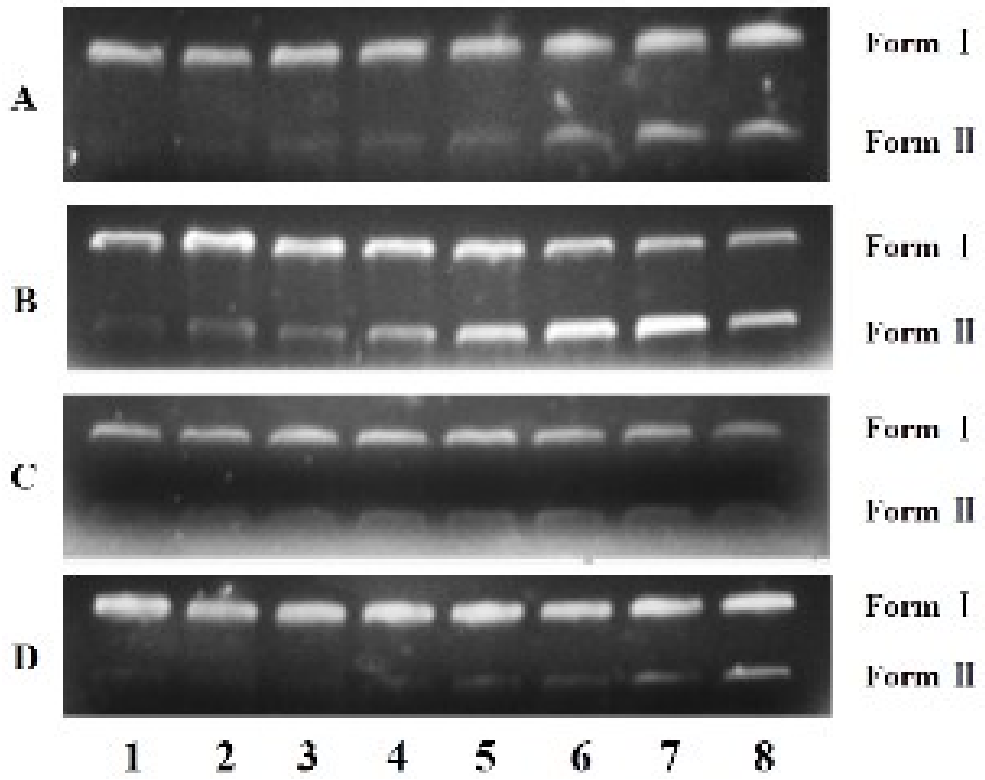

Fig. S14 Cleavage of pUC19 DNA (0.1 μg μL^{-1}) with different concentrations of complex **1** (A), **2** (B), **3** (C) and **4** (D) after 3 h incubation at 37 °C in Tris-HCl/NaCl buffer (pH = 7.2). Lane 1: DNA control; lanes 2–8: DNA + complex (50, 100, 175, 250, 325, 400 and 450 μM), respectively.

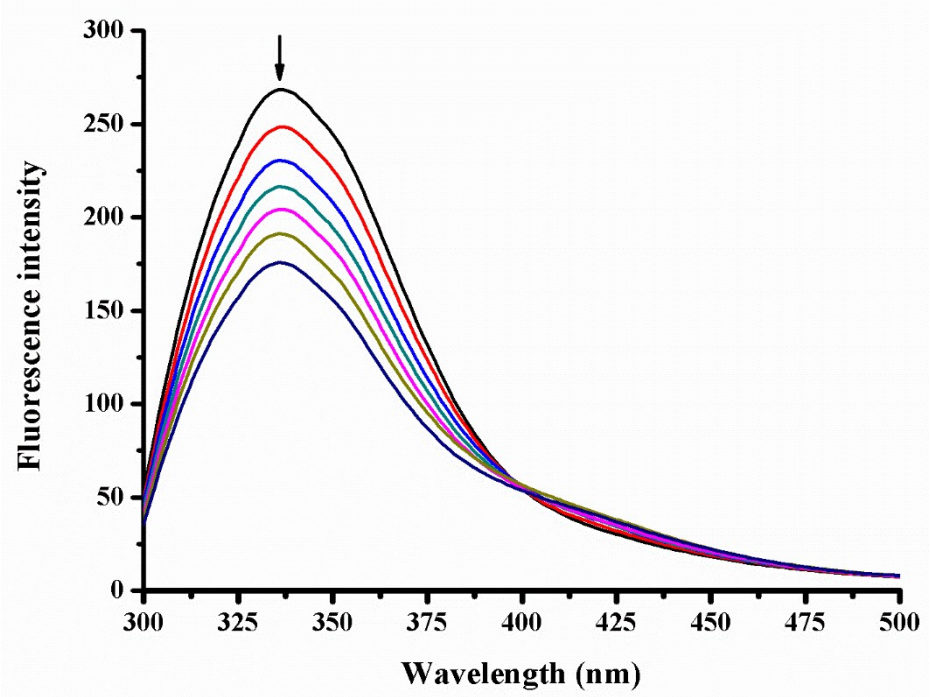

Fig. S15 Fluorescence spectra of HSA in the increasing concentration of complex **2** at room temperature. The concentration of HSA is 0.25 μM, and Complexes are (0 – 12 μM).

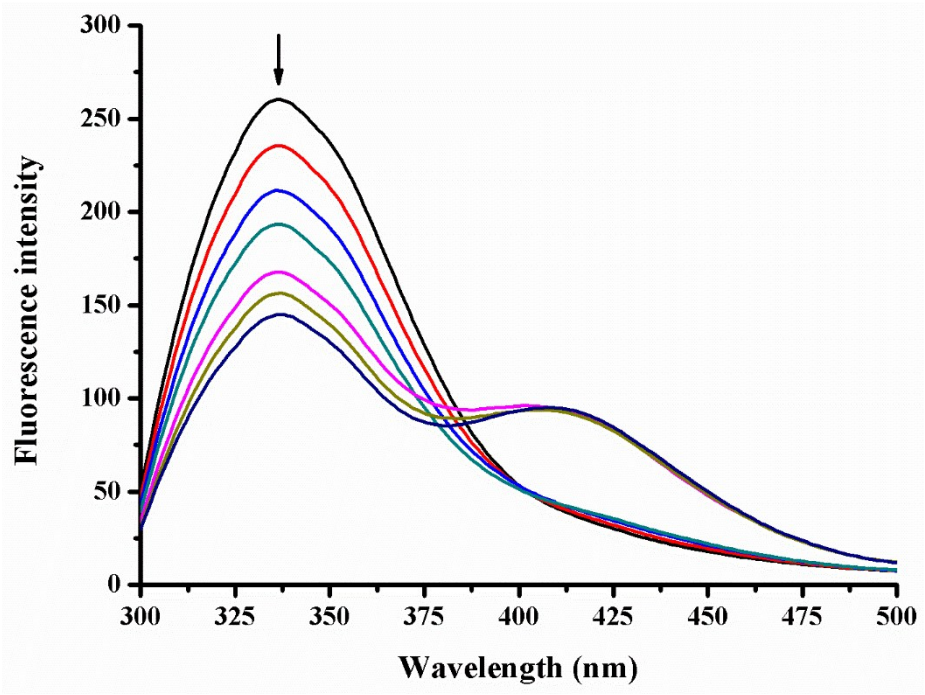

Fig. S16 Fluorescence spectra of HSA in the increasing concentration of complex **3** at room temperature. The concentration of HSA is 0.25 μM, and Complexes are (0 – 12 μM).

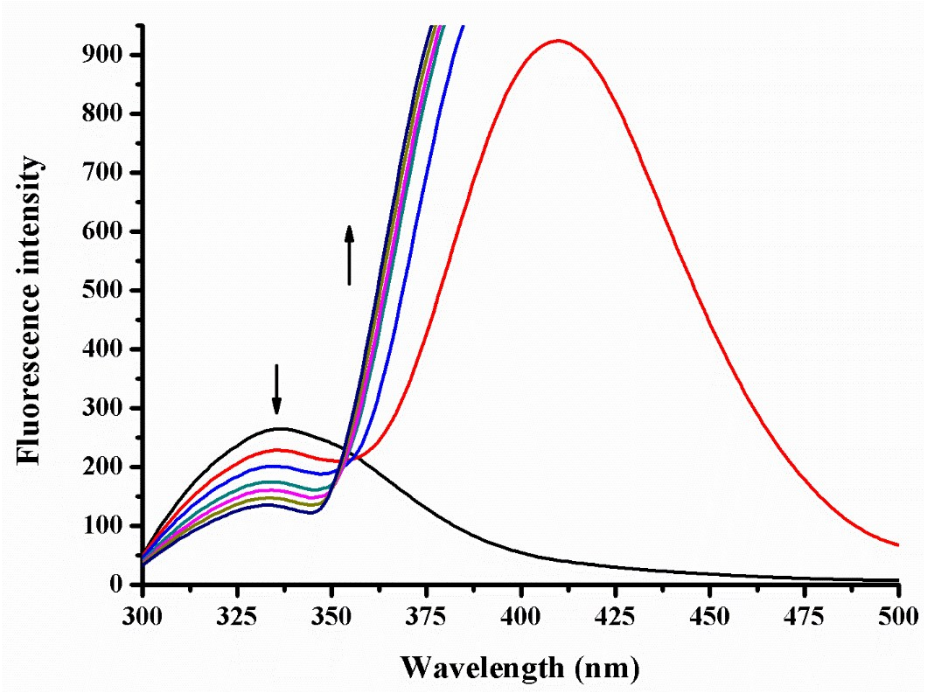

Fig. S17 Fluorescence spectra of HSA in the increasing concentration of complex **4** at room temperature. The concentration of HSA is 0.25 μM, and Complexes are (0 – 12 μM).

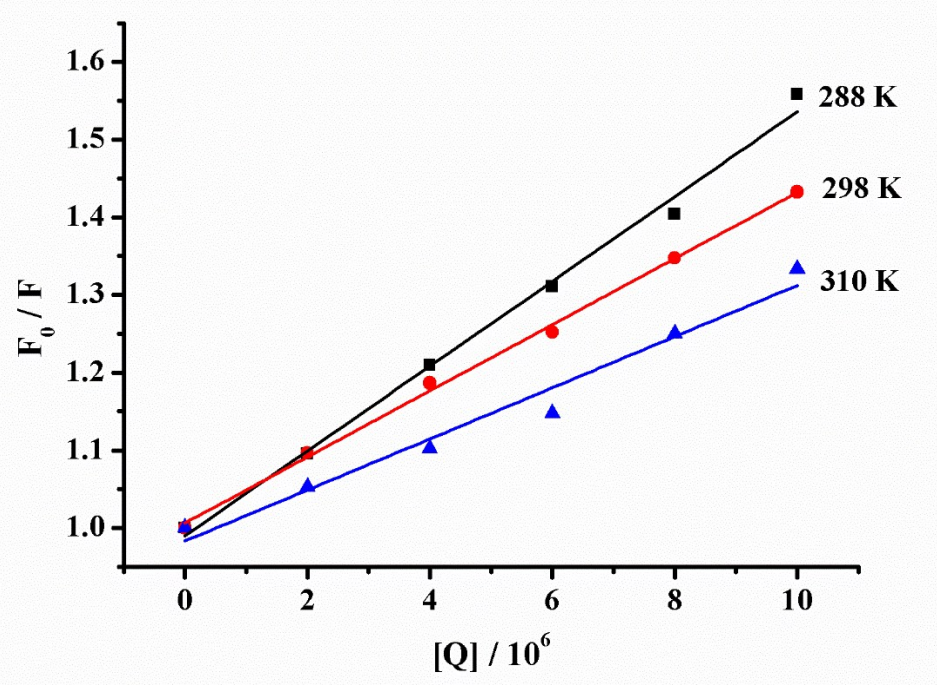

Fig. S18 The Stern-Volmer plots of the fluorescence quenching of HSA by complex **2** at different temperature (T = 288, 298 and 310 K).

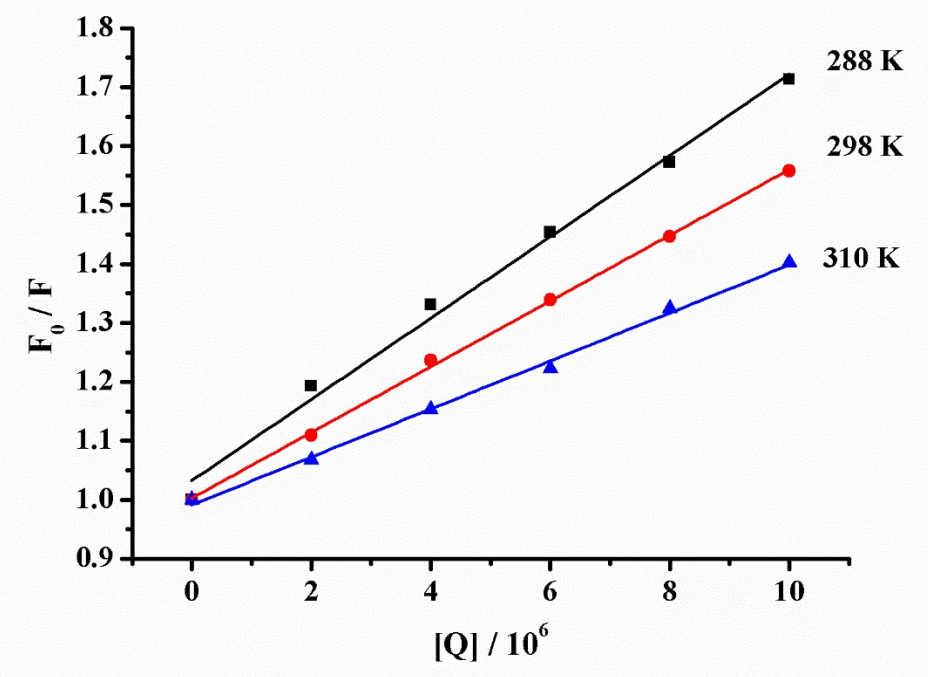

Fig. S19 The Stern-Volmer plots of the fluorescence quenching of HSA by complex **3** at different temperature (T = 288, 298 and 310 K).

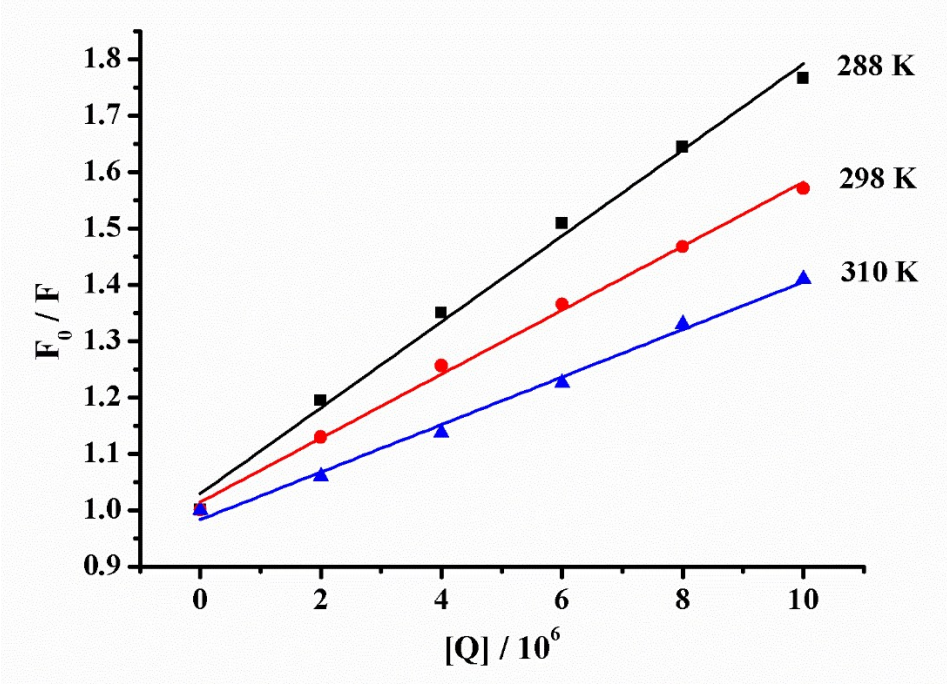

Fig. S20 The Stern-Volmer plots of the fluorescence quenching of HSA by complex **4** at different temperature (T = 288, 298 and 310 K).

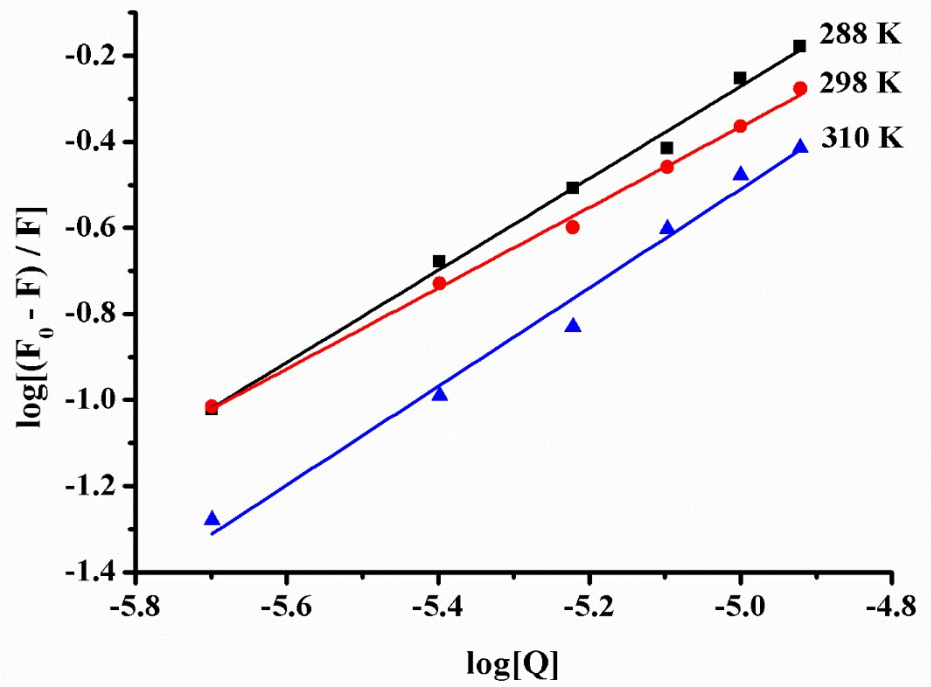

Fig. S21 The plots of log [(F_0-F)/F] vs. log [Q] of HSA at different temperature (T = 288, 298, 310 K) for complex **2**.

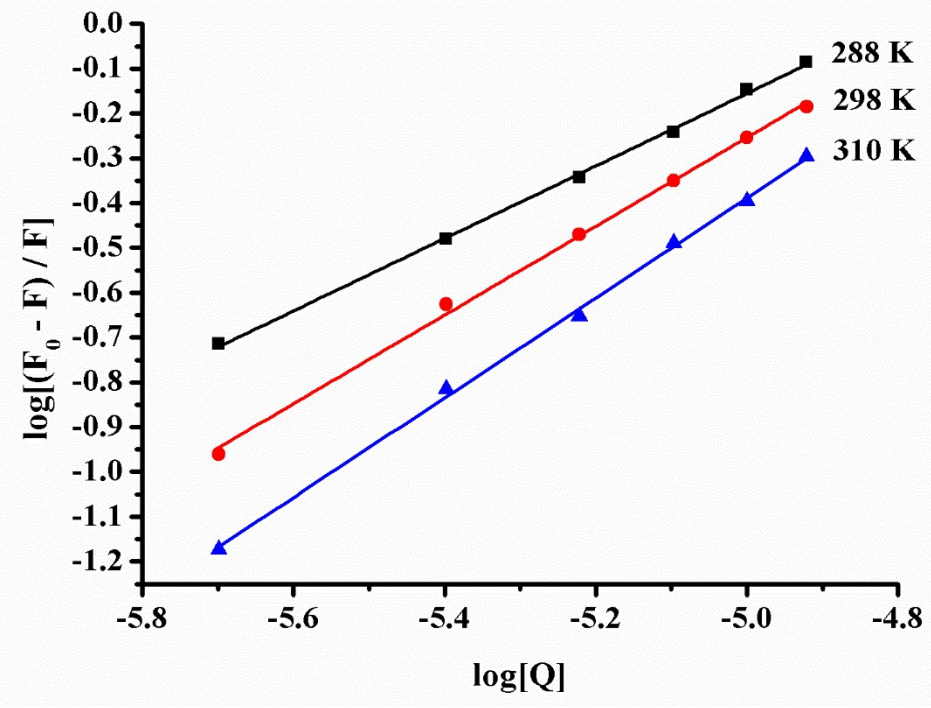

Fig. S22 The plots of log [(F_0-F)/F] vs. log [Q] of HSA at different temperature (T = 288, 298, 310 K) for complex **3**.

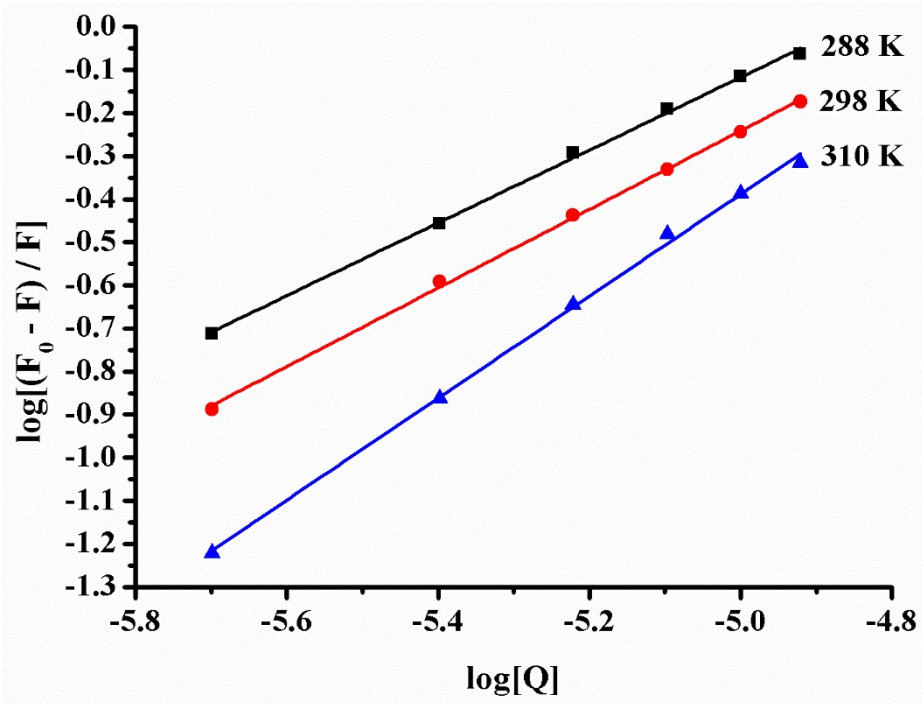

Fig. S23 The plots of log [(F_0-F)/F] vs. log [Q] of HSA at different temperature (T = 288, 298, 310 K) for complex **4**.

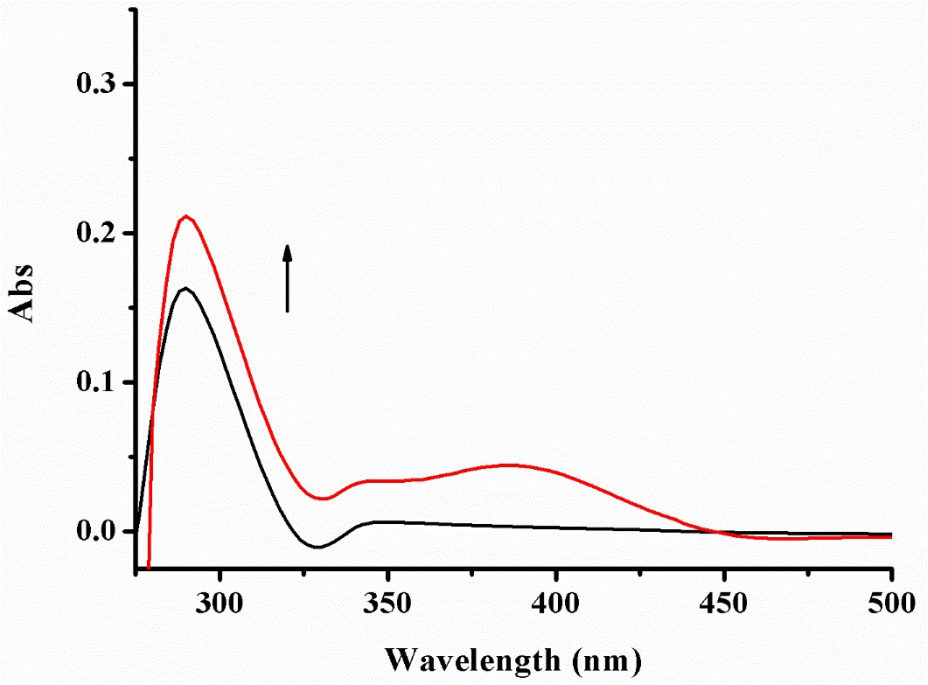

Fig. S24 UV-vis absorption spectra of HSA in the absence and presence of complex **2.** Black line: the absorption of BSA. Red line: the absorption of HSA in the presence of complex **2** at the same concentration, c (BSA) = c (complex **2**) = 10 μM.

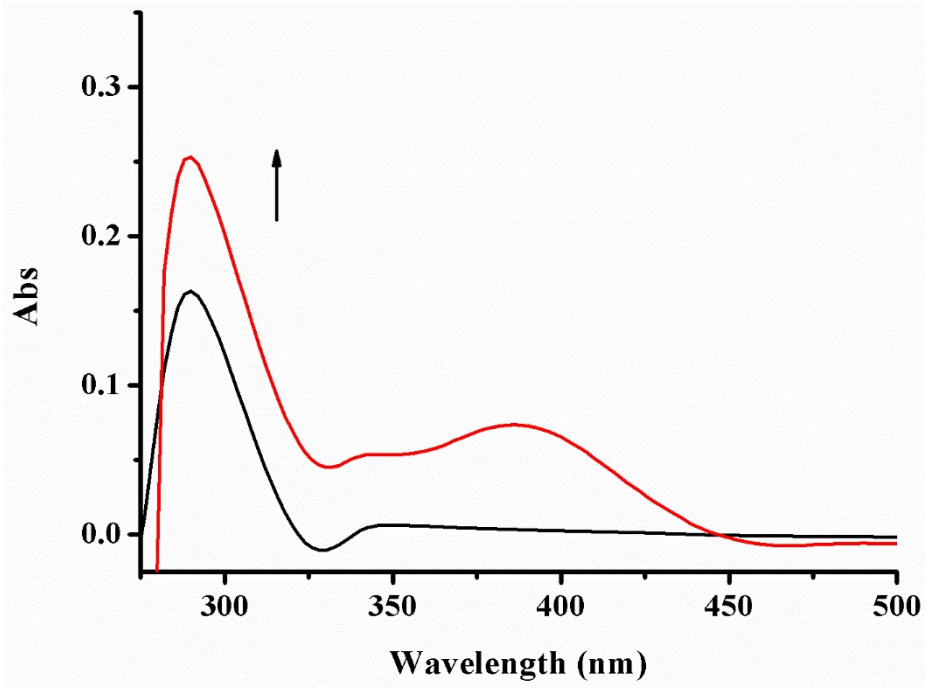

Fig. S25 UV-vis absorption spectra of HSA in the absence and presence of complex **3.** Black line: the absorption of BSA. Red line: the absorption of HSA in the presence of complex **3** at the same concentration, c (BSA) = c (complex **3**) = 10 μM.

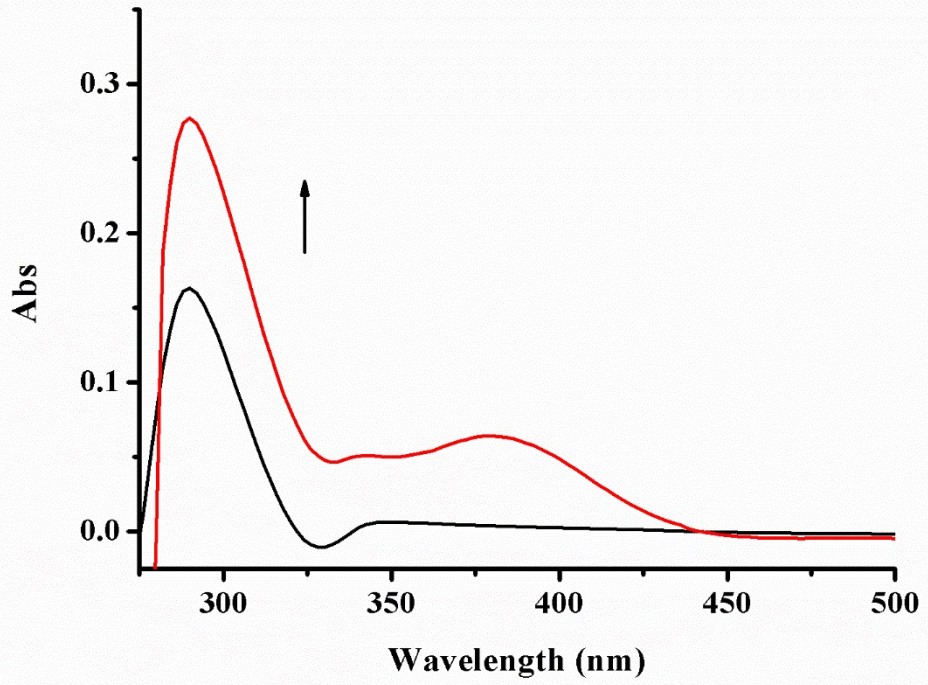

Fig. S26 UV-vis absorption spectra of HSA in the absence and presence of complex **4.** Black line: the absorption of BSA. Red line: the absorption of HSA in the presence of complex **4** at the same concentration, c (BSA) = c (complex **4**) = 10 μM.

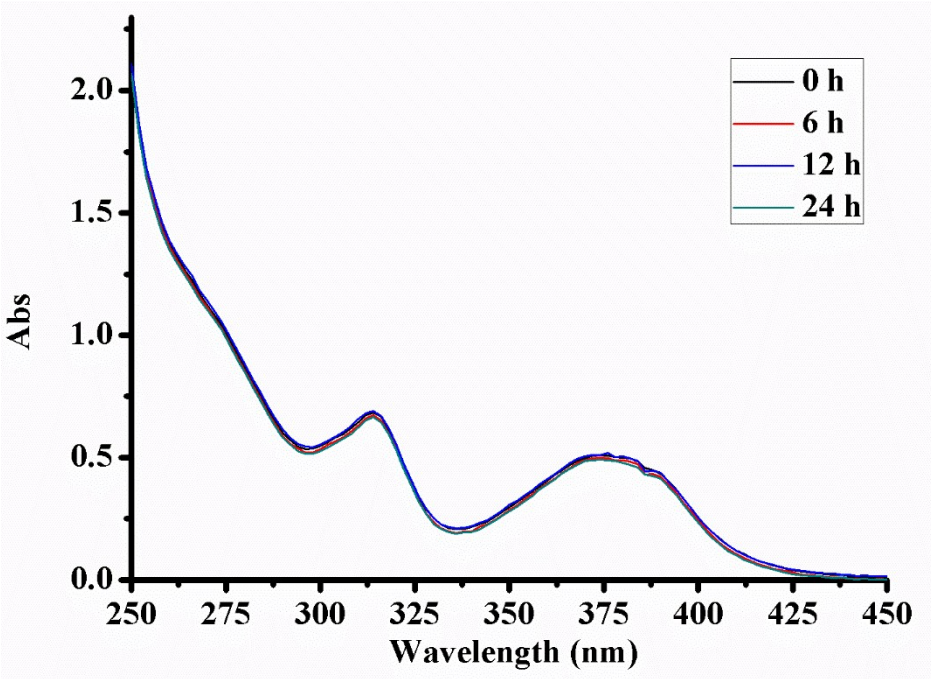

Fig. S27 Absorption spectra of complex **1** (80 μM) at 0 h, 6 h, 12 h, 24 h at 37 ℃ in PBS buffer.

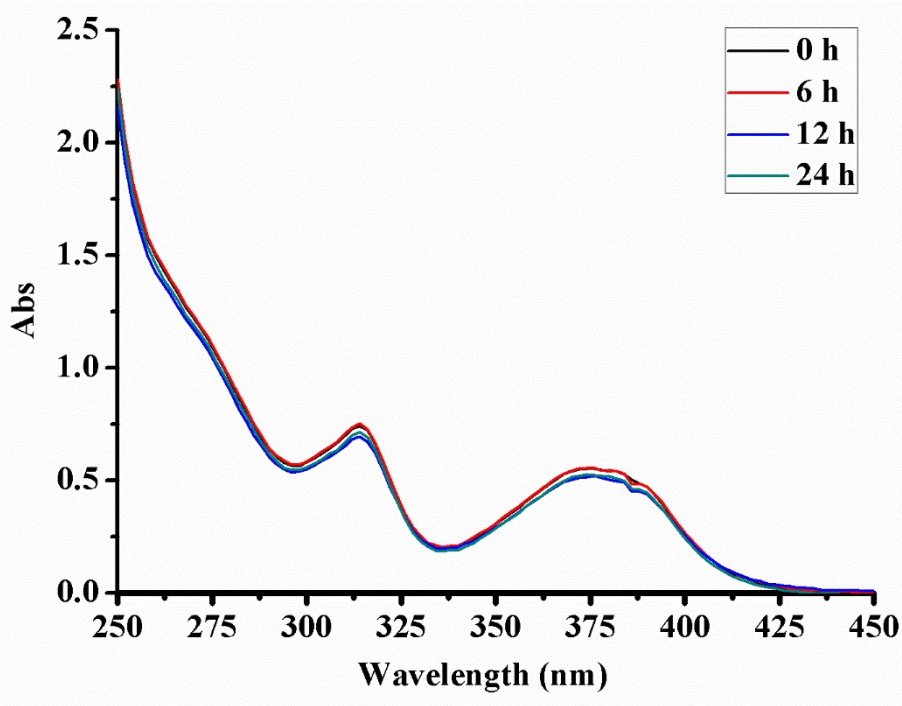

Fig. S28 Absorption spectra of complex **2** (80 μM) at 0 h, 6 h, 12 h, 24 h at 37 ℃ in PBS buffer.

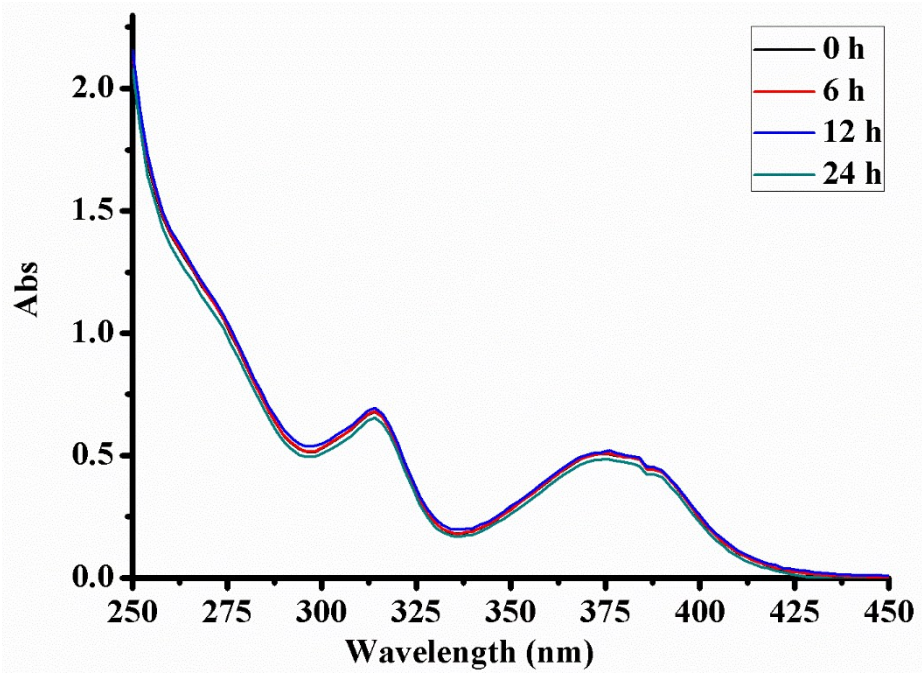

Fig. S29 Absorption spectra of complex **3** (80 μM) at 0 h, 6 h, 12 h, 24 h at 37 ℃ in PBS buffer.

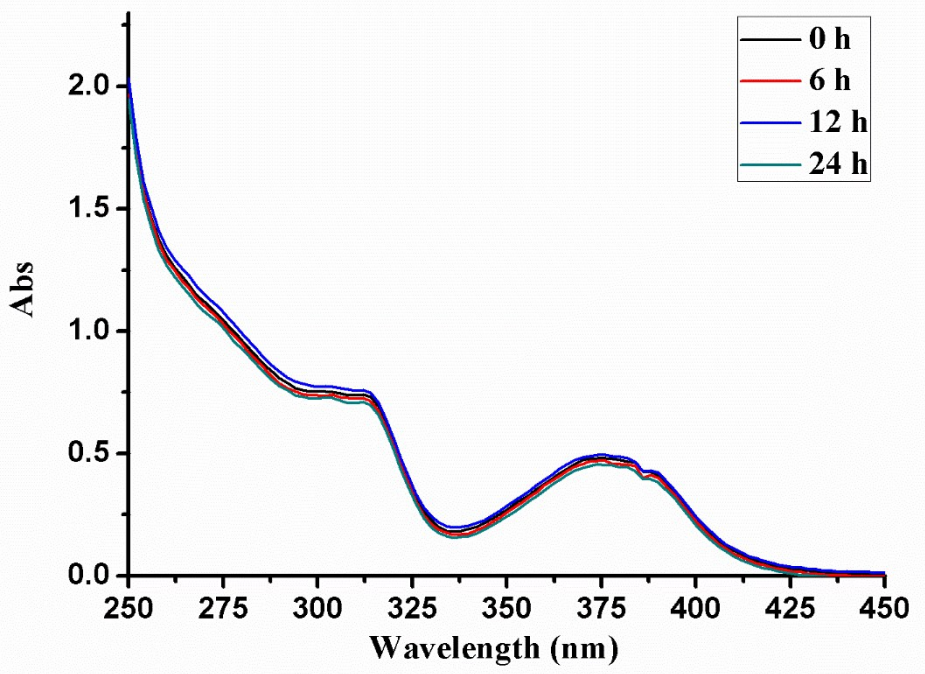

Fig. S30 Absorption spectra of complex **4** (80 μM) at 0 h, 6 h, 12 h, 24 h at 37 ℃ in PBS buffer.

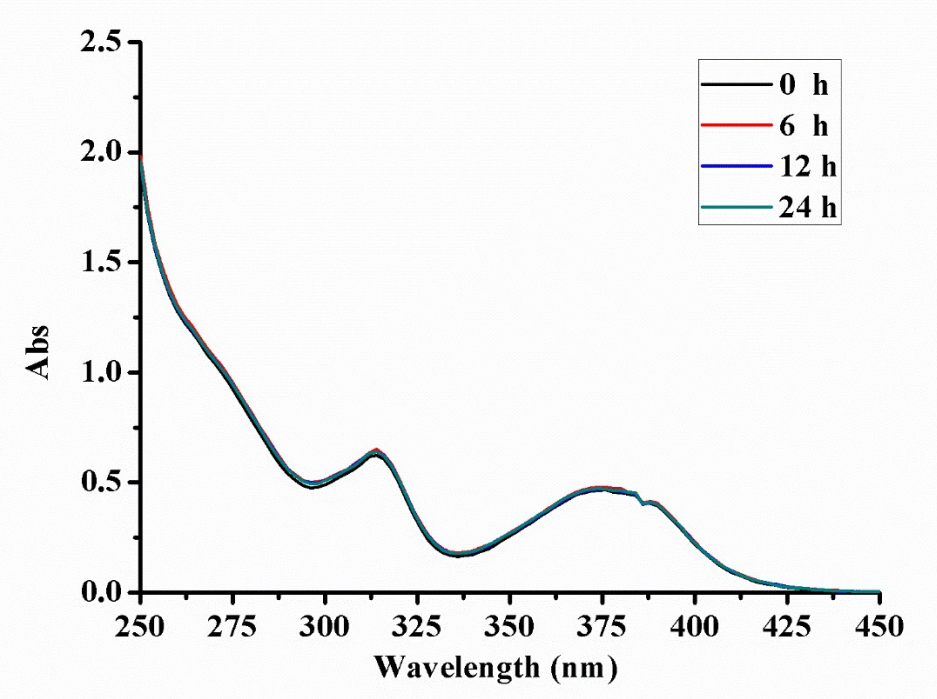

Fig. S31 Absorption spectra of complex **1** (80 μM) at 0 h, 6 h, 12 h, 24 h at 37 ℃ in Tris buffer.

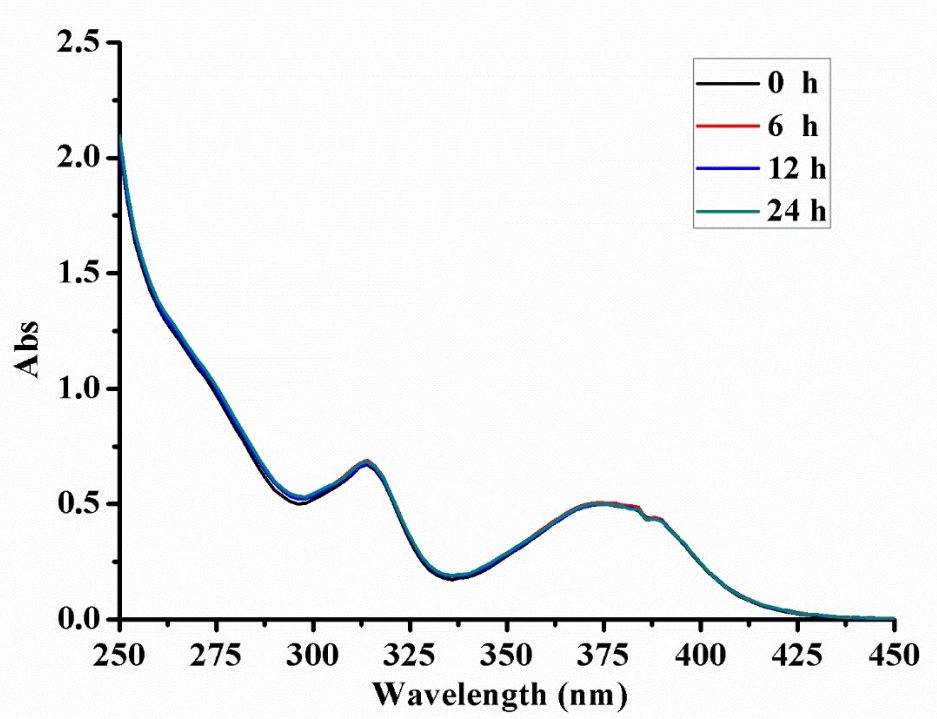

Fig. S32 Absorption spectra of complex **2** (80 μM) at 0 h, 6 h, 12 h, 24 h at 37 ℃ in Tris buffer.

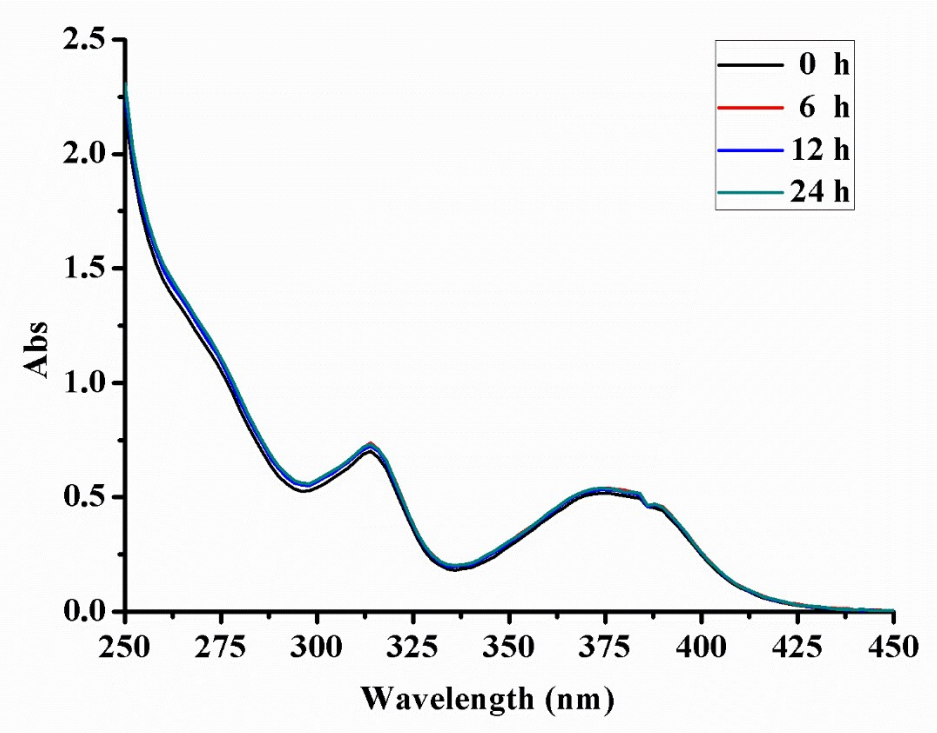

Fig. S33 Absorption spectra of complex **3** (80 μM) at 0 h, 6 h, 12 h, 24 h at 37 ℃ in Tris buffer.

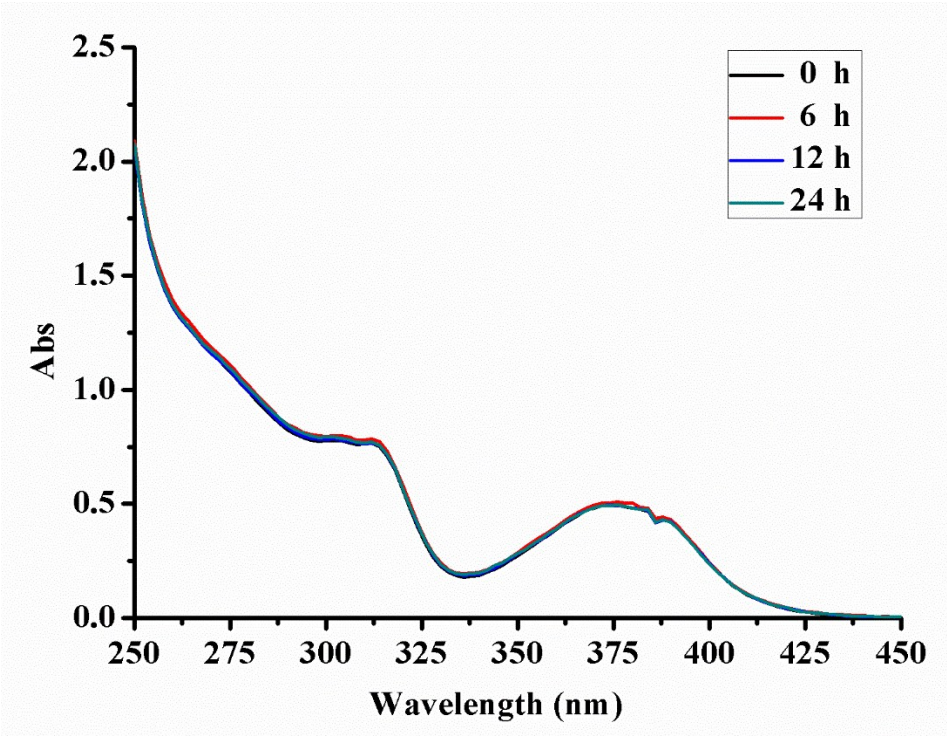

Fig. S34 Absorption spectra of complex **4** (80 μM) at 0 h, 6 h, 12 h, 24 h at 37 ℃ in Tris buffer.